Synthesis, X-ray structure, electrochemical and electronic properties of [3-(pyridin-2-yl)-4-methyl-1,2,4-triazole-bis(2-(2′-phenylato)pyridine)-iridium(III)] hexafluorophosphate

J. H. van Diemen, J. G. Haasnoot*, R. Hage, E. Müller and **J. Reedijk**
Department of Chemistry, Gorlaeus Laboratories, Leiden University, P.O. Box 9502, 2300 RA Leiden (The Netherlands)

(Received October 8, 1990)

Abstract

A new orthometalated iridium(III) complex $[Ir(ppy)_2(4mptr)](PF_6)$ with ppy = 2-(2′-phenylato)pyridine and 4mptr = 4-methyl-3-(pyridin-2-yl)-1,2,4-triazole has been synthesised and characterised by X-ray structure analysis, NMR spectroscopy, electrochemical measurements, UV–Vis absorption, and emission spectroscopy. The compound crystallises in the orthorhombic space group *Pbca*, with $a = 10.906(4)$, $b = 16.139(6)$, $c = 32.876(12)$ Å and $Z = 8$. The cation has a distorted octahedral IrN_4C_2 chromophore, with two chelating (C,N) ppy ligands ($\langle Ir\text{–}C \rangle = 2.01$ Å, $\langle Ir\text{–}N \rangle = 2.05$ Å). The two carbon atoms are *cis* and the two nitrogen atoms *trans* to each other. The 4mptr ligand chelates via the pyridine nitrogen (Ir–N13 = 2.18 Å) and N2 of the triazole ring (Ir–N2 = 2.14 Å), both *trans* to a carbon atom. The complex is reversibly reduced in CH_3CN at −1.57 V (SCE) and irreversibly oxidised at +1.20 V (SCE). The lowest UV–Vis absorption band at 380 nm ($\epsilon = 5400$) has been assigned to a $d \rightarrow \pi^*$ (ppy) MLCT transition. A highly-structured emission band (471/505 nm) is observed at 77 K, while at room temperature, only a broad emission (582 nm) is present.

Introduction

In contrast to the extensively studied polypyridylruthenium(II) systems, considerable less research has been carried out on analogous orthometalated (cyclometalated) d^6 and d^8 transition metal complexes [1–5]. Interesting excited-state properties may be obtained for such metal complexes by introducing an orthometalated ligand adjacent to bpy-type ligands [6–8]. The strong σ-donor properties of the negatively-charged ligands result in distinct electronic structures and redox properties.

Recently, the electrochemical and photophysical properties of Pd(II) [9, 10], Pt(II) [11–14], Rh(III) [15–18] and Ir(III) [6, 17, 19] complexes containing orthometalated (NC) ligands like 2-phenylpyridine (Hppy) and benzo(h)quinoline (bzq) have been investigated. They show significant differences in excited-state properties compared to their isostructural 2,2′-bipyridine (bpy) and 1,10-phenanthroline (phen) analogues. Compounds of the formulae $Ru(bpy)_2(L)$ and $Os(bpy)_2(L)$ containing pyridyltriazole ligands have previously been studied in our laboratory [20–26]. To investigate the influence of a metal–carbon bond next to metal–nitrogen bonds in the triazole-containing systems, some $Rh(ppy)_2(L)$ complexes with (non-)substituted pyridyltriazoles have recently been synthesised and characterised [27]. In this paper, we report about an orthometalated $Ir(ppy)_2(L)$ complex and compare it with analogous orthometalated Ir(III) and Rh(III) complexes (Scheme 1).

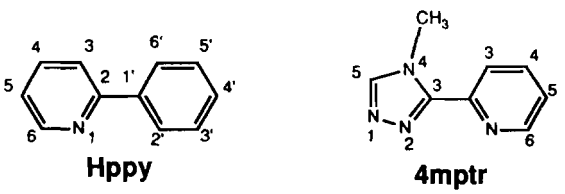

Scheme 1. Ligands with atomic numbering.

Experimental

Materials

Iridium trichloride and 2-phenylpyridine were obtained from Janssen Chimica and used without further purification. The ligand 4-methyl-3-(pyridin-2-yl)-1,2,4-triazole (4mptr) was synthesised and characterised as previously reported [28]. The starting

*Author to whom correspondence should be addressed.

0020-1693/91/$3.50

material, $[Ir(ppy)_2Cl]_2$, was prepared as reported for the rhodium analogue [27].

Preparation of [Ir(ppy)$_2$(4mptr)](PF$_6$)

$[Ir(ppy)_2Cl]_2$ (0.25 mmol) and 0.65 mmol of the ligand were heated to reflux in 2-methoxyethanol for 48 h. After cooling to room temperature the solution was evaporated to 10 ml and added to an excess of aqueous NH_4PF_6. The resulting precipitate was filtered off and recrystallised from water/acetone (1/1).

Anal. Calc. for $[Ir(C_{30}H_{24}N_6)]PF_6$: C, 44.72; H, 3.00; N, 10.43; P, 3.84. Found: C, 44.97; H, 3.16; N, 10.46; P, 3.71%.

Physical measurements

Proton NMR spectra were recorded on a Jeol JNM-FX 200 MHz spectrometer or a Bruker 300 MHz spectrometer. All peak positions are relative to TMS.

For the COSY experiment 256 FIDs of eight scans each, consisting of 1 K data points, were accumulated. After digital filtering (sine bell squared), the FID was zero filled to 512 W in the F_1 dimension. Aquisition parameters were $F_1 = 500$ Hz and $t = 0.001$ s; the cycle decay was 1.5 s.

Electronic absorption spectra were recorded in ethanol on a Perkin-Elmer 330 UV–Vis spectrophotometer and a Varian DMS 200 UV–Vis spectrophotometer using 1 cm quartz cells.

Emission spectra were obtained on a Perkin-Elmer LS-5 luminescence spectrometer, equipped with a red-sensitive Hamamatsu R928 detector. Emission wavelengths are not corrected for photomultiplier response.

The differential pulse polarographic measurements were carried out on an EG&G PAR C model 303 with an EG&G 384B polarographic analyser. The scan rate was 4 mV/s with a pulse height of 20 mV. A saturated calomel electrode (SCE) was used as a reference electrode; all measurements were carried out using a platinum electrode. The solvent was CH_3CN (spectroscopic grade) containing 0.1 M tetrabutylammonium perchlorate (TBAP) as supporting electrolyte. The solutions were purged with argon before all measurements.

Elemental analyses (C, H, N, and P) were carried out at University College Dublin.

X-ray crystallography

A yellow, bar-shaped crystal of dimensions $0.35 \times 0.10 \times 0.05$ mm was selected for X-ray analysis and mounted in a Lindemann capillary. Crystal and data collection parameters are summarised in Table 1. Data collection took place on an Enraf-Nonius CAD-4-diffractometer at room temperature. Cell parameters were determined from 24 reflections with $10 < \theta < 11°$. Periodic orientation and intensity controls during measurements did not indicate any crystal decomposition. A total of 8426 unique reflections was measured with $2 < \theta < 30°$. Data were reduced and corrected for Lorentz and polarisation effects, using local programs [29]. Absorption correction was based on ψ-scan data of the $(-8,0,0)$ reflection [30].

TABLE 1. Crystallographic data for [Ir(ppy)$_2$(4mptr)](PF$_6$)

Chemical formula	$IrC_{30}H_{24}N_6PF_6$
Molecular weight	805.75
Space group	*Pbca* (orthorhombic)
Z	8
Volume (Å^3)	5789.5
a (Å)	10.906(4)
b (Å)	16.139(6)
c (Å)	32.876(12)
D_c (g cm^{-3})	1.837
D_m (g cm^{-3})	1.825
μ (cm^{-1})	4.6
$F(000)$	3135
λ(Mo Kα) (Å)	0.71069
Scan type	$\omega/2\theta$
θ range (°)	2–30
No. unique reflections	8426
R_{int}	0.021
No. of reflections used in refinement	3103 ($I > 1.5\sigma(I)$)
No. variables	422
R	0.040
R_w	0.044

The structure was solved with direct methods (SHELXS-86) [31] and refined and completed in SHELX76 [32]. The final refinement (unit weights) converged to an R value of 3.97% with 3103 observations ($F > 3\sigma_F$) and 422 parameters. All non-hydrogen atoms were refined anisotropically; the hydrogen atoms were put in calculated positions and allowed to ride on the corresponding carbon atoms. Isotropic temperature factors were refined individually for all hydrogen atoms. The final difference Fourier map showed a ring of residual electron density with a maximal height of 1.3 e/Å at a distance of about 1 Å around the Ir atom. Such a feature is, however, expected due to series termination errors in the structure factor.

Scattering factors were taken from the International Tables for X-ray Crystallography [33]. Final fractional atomic coordinates and isotropic thermal parameters for the non-hydrogen atoms are given in Table 2.

TABLE 2. Atomic fractional coordinates ($\times 10^5$ for Ir; $\times 10^4$ for the other atoms) and isotropic temperature factors ($\times 10^4$ for Ir; $\times 10^3$ for the other atoms) of $[Ir(ppy)_2(4mptr)](PF_6)$

Atom	x/a	y/b	z/c	B_{iso}
Ir	3926(4)	448(3)	35518(1)	346(2)
P	5463(5)	3345(3)	424(1)	73(3)
F1	5664(17)	4220(9)	604(6)	180(15)
F2	6826(12)	3271(10)	411(7)	205(17)
F3	5474(16)	3735(13)	8(4)	219(17)
F4	5415(15)	2978(9)	859(4)	160(12)
F5	5278(17)	2474(10)	278(5)	201(16)
F6	4085(11)	3432(12)	453(6)	200(17)
N1	388(12)	−983(8)	4406(4)	62(8)
N2	802(9)	−351(7)	4166(3)	45(1)
C3	1550(10)	151(11)	4374(4)	53(8)
C4	2269(20)	131(18)	5111(5)	126(18)
N4	1594(12)	−164(12)	4775(4)	86(11)
C5	831(15)	−891(10)	4772(5)	64(10)
N13	1711(10)	951(7)	3779(4)	49(7)
C14	2116(12)	850(10)	4166(5)	55(9)
C15	2995(16)	1371(12)	4337(9)	93(16)
C16	3463(19)	1930(12)	4128(10)	110(20)
C17	3114(16)	2026(10)	3723(7)	74(9)
C18	2226(12)	1538(8)	3548(6)	58(9)
C20	−826(11)	−843(8)	3421(3)	40(6)
C21	−2042(10)	−652(7)	3563(4)	45(7)
C22	−3005(14)	−1205(9)	3497(5)	62(10)
C23	−2814(16)	−1934(10)	3296(6)	77(12)
C24	−1640(15)	−2137(9)	3167(5)	67(9)
C25	−676(13)	−1604(8)	3231(4)	50(7)
N26	−1140(9)	598(7)	3795(3)	41(6)
C27	−2203(10)	150(9)	3763(3)	43(7)
C28	−3295(13)	487(10)	3912(4)	59(9)
C29	−3303(15)	1246(11)	4094(5)	71(11)
C30	−2214(15)	1681(10)	4126(5)	65(9)
C31	−1163(13)	1343(9)	3968(4)	51(8)
C40	128(11)	485(7)	2994(4)	39(6)
C41	976(11)	185(7)	2704(3)	40(6)
C42	901(13)	407(9)	2297(4)	53(8)
C43	−9(13)	945(10)	2170(4)	60(9)
C44	−835(14)	1260(9)	2447(5)	58(8)
C45	−766(12)	1032(8)	2855(4)	48(7)
N46	1832(9)	−520(6)	3269(3)	38(5)
C47	1921(12)	−390(8)	2863(3)	41(6)
C48	2863(13)	−756(8)	2648(4)	53(8)
C49	3697(12)	−1250(9)	2833(4)	59(9)
C50	3604(12)	−1376(9)	3248(4)	51(8)
C51	2662(11)	−1010(8)	3456(4)	44(7)

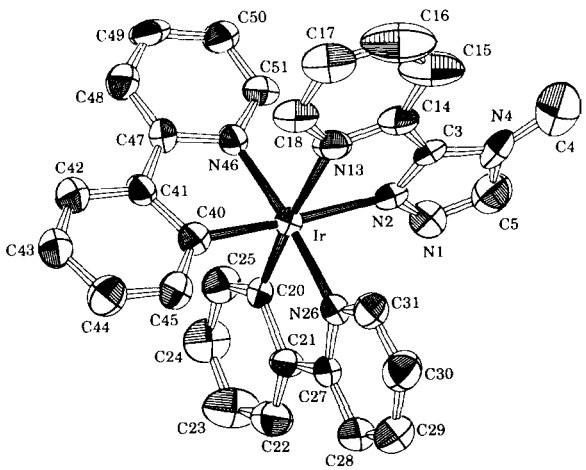

Fig. 1. ORTEP [34] drawing with atomic numbering of $[Ir(ppy)_2(4mptr)]^+$ in 50% probability; Hydrogen atoms are omitted for clarity.

Results and discussion

Description of the X-ray structure

As presented in Fig. 1, the Ir(III) ion has an octahedral coordination containing four nitrogen and two carbon atoms. Relevant bond distances and angles for the title compound are shown in Table 3. The Ir–C and Ir–N distances for the ppy ligands, 2.01 and 2.05 Å, respectively, are similar to those observed in analogous orthometalated rhodium(III) complexes [35, 36] and agree with earlier reported standard values [37]. Such observations have been made for $[Ir(bpy)_3]^{3+}$ and $[Rh(bpy)_3]^{3+}$: the metal–nitrogen bond lengths are the same for both complexes within experimental error [38, 39]. This has been observed [40, 41] for $[Ru(bpy)_3]^{2+}$ and $[Os(bpy)_3]^{2+}$, which has been explained by the fact that at first the diffuse 4f orbitals have to be filled for the third transition metal series, before the 5d orbitals are occupied [42, 43]. The coordination geometry of the ppy ligands around the metal ion, i.e. with the metal–carbon in a mutual *cis* orientation is in agreement with earlier results reported Rh [17, 27, 35]. As is seen in Fig. 1, the pyridyltriazole ligand (4mptr) is coordinated to the metal ion via N2 of the triazole ring (2.139(10) Å) and N13 of the pyridyl ring (2.175(11) Å). No literature data are available for similar orthometalated Ir(III) complexes, although a chloro-bridged iridium dimer containing the cyclometalated ligand 2-(p-tolyl)pyridine has been synthesised [17]. Compared with Rh(III) complexes, synthesised recently [27], a remarkable difference is observed. The Ir–N(triazole) distance appears to be significantly shorter than the Rh–N(triazole) bond length observed for $[Rh(ppy)_2(L)]^+$ with L = 5-phenyl-3-(pyridin-2-yl)-1,2,4-triazole and 3-(pyridin-2-yl)-5-(2-thienyl)-1,2,4-triazole [27, 44]. This difference can be understood by comparing the possible coordination modes for triazole ligand systems. Previous work on bis(pyridyl)ruthenium(II) complexes containing various pyridyltriazoles revealed that two coordination modes can be present, namely via N1 (N2) or N4 of the triazole ring [45]. X-ray structure determinations showed that the Ru–N1 (N2) bond

TABLE 3. Selected bond distances (Å) and angles (°) for $[Ir(ppy)_2(4mptr)](PF_6)$

Ir–N2	2.139(10)	N1–N2	1.37(2)	N1–N2–C3	111(1)
Ir–N13	2.175(11)	N2–C3	1.34(2)	N2–C3–N4	106(1)
Ir–N26	2.046(11)	C3–N4	1.41(2)	C3–N4–C4	129(2)
Ir–N46	2.051(9)	C4–N4	1.41(2)	C3–N4–C5	106(1)
Ir–C20	2.007(13)	N4–C5	1.44(2)	C4–N4–C5	126(2)
Ir–C40	2.011(12)	N1–C5	1.31(2)	C5–N1–C2	109(1)
		C3–C14	1.46(2)	N4–C5–N1	108(1)
N13–Ir–N2	75.7(4)	C14–C15	1.39(2)	N2–C3–C14	119(1)
C20–Ir–N2	97.9(4)	C15–C16	1.24(3)	N4–C3–C14	135(1)
C20–Ir–N13	173.6(4)	C16–C17	1.39(3)	C3–C14–N13	113(1)
N26–Ir–N2	87.1(4)	C17–C18	1.38(2)	C3–C14–C15	125(2)
N26–Ir–N13	97.0(4)	C18–N13	1.34(2)	C14–C15–C16	120(2)
N26–Ir–C20	81.8(5)	N13–C14	1.36(2)	C14–N13–C18	119(1)
C40–Ir–N2	175.1(4)			C15–C16–C17	120(2)
C40–Ir–N13	99.5(5)			C15–C14–N13	122(2)
C40–Ir–C20	86.9(5)			C16–C17–C18	122(2)
C40–Ir–N26	94.4(4)			N13–C17–C18	118(2)
N46–Ir–N2	98.1(4)				
N46–Ir–N13	87.0(4)				
N46–Ir–C20	94.8(4)				
N46–Ir–N26	174.1(4)				
N46–Ir–C40	80.6(4)				

length is significantly shorter than the Ru–N4 distance, due to differences in σ-donor properties of N1 (N2) versus N4 [46].

In the case of the two above-mentioned rhodium complexes the triazole ring is bound via N4, although coordination via N2 would also be possible. The N4 coordination mode seems to be favoured compared to N1 (N2), most likely due to electronic effects [27]. For the iridium complex only one coordination mode (N2) is possible, while the N4 site is now blocked by a methyl substituent. So, the triazole ring is bound via the strongest σ-donor site resulting in a rather short Ir–N(triazole) bond as compared to the Rh–N(triazole) distances. The bite angles of the ppy ligands and 4mptr, 81.8(5), 80.6(5) and 75.7(4)° respectively, lie in the same range as observed before [22, 24, 27].

NMR spectroscopy

NMR techniques, especially 2D-techniques (COSY), have proven to be important in elucidating the structure of polypyridyl d^6 transition metal complexes. Although the NMR data are not essential for the structure determination of the title compound, a few comments should be made considering the NMR results (Fig. 2 and Table 4).

(i) A large upfield shift (−0.68 ppm) for the H6 proton of the 4mptr ligand is observed. This shift is caused by a considerable magnetic interaction between the H6 proton and a pyridine ring of one of the ppy ligands.

(ii) A separation of the two H6 (ppy) resonance signals is observed, which can be explained by the difference in shielding. One of the H6 protons is in the shielding cone of the pyridine ring of the 4mptr ligand, while the H6 proton of the other ppy ligand interacts with the triazole ring system.

(iii) Compared to the rhodium equivalent, $[Rh(ppy)_2(4mptr)](PF_6)$, an upfield shift of 0.1–0.2 ppm for all protons is observed. The reason for this difference, which has also been found in the case of $Ru(bpy)_2(L)$ versus $Os(bpy)_2(L)$ with L a substituted pyridyltriazole [46, 47], is not yet understood.

(iv) A difference in chemical shifts for the protons (H3′–H6′) of the two phenyl rings has been found. This can be explained by considering the ligands *trans* positioned to the phenyl ring. As is clear from Fig. 2, the pyridyl N13 atom and triazole N2 atom are *trans* towards C20 and C40, respectively. While the σ-donor properties of N2 are much stronger than those of N13, the change in electron density will be larger for the C20–C25 phenyl ring.

Electrochemistry

The redox data for the title compound are depicted in Table 5. As pointed out before, the oxidation processes of orthometalated complexes is caused by removal of metal-localised electrons. For the iridium complex, one (irreversible) oxidation wave is observed at 1.20 V. This oxidation is shifted to lower potential compared to that of $[Ir(ppy)_2(bpy)](PF_6)$ [48], which suggests that the charge density on the metal ion is higher in the case of the triazole-containing monomer. The stronger σ-donor capability of the triazole ring system with respect to bpy is most likely to be responsible for this difference in oxidation potential.

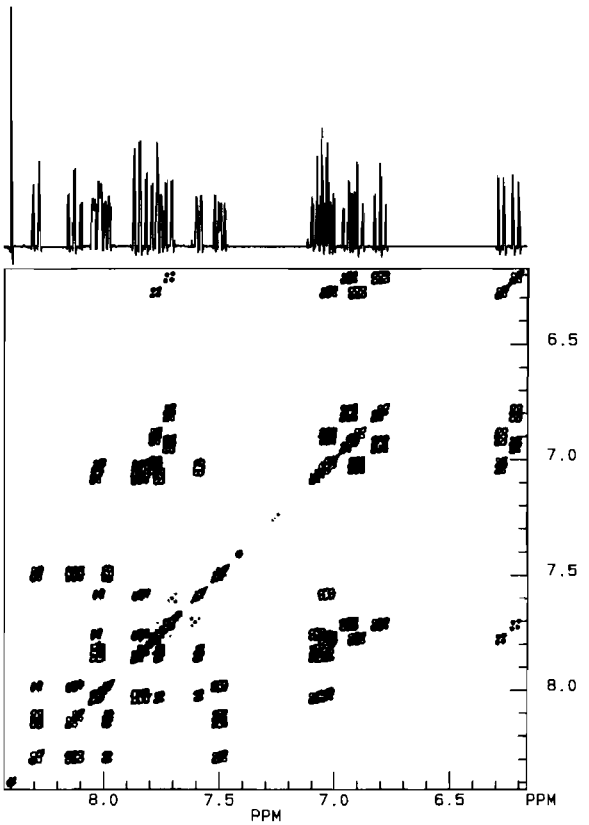

Fig. 2. COSY NMR spectrum of $[Ir(ppy)_2(4mptr)](PF_6)$ measured in CD_3CN.

TABLE 4. ^1H NMR proton resonance signals (in ppm vs. TMS) of $[Ir(ppy)_2(4mptr)](PF_6)$ measured in CD_3CN

ppy Ligand				4mptr Ligand[a]	
H3′	6.22+6.28	H3	8.04	H3	8.30(+0.19)
H4′	6.81+6.92	H4	7.85	H4	8.13(+0.18)
H5′	6.95+7.04	H5	7.06	H5	7.50(+0.03)
H6′	7.72+7.78	H6	7.59+7.76	H6	7.98(−0.68)
				CH_3	4.25(+0.27)
				H5(tr)	8.41(−0.21)

[a]Figures in parentheses are shifts compared to the free ligand, those to lower field being positive.

The first reduction wave is observed at −1.57 V versus SCE and appeared to be reversible. Compared to the bpy analogue (a bpy-based reduction at −1.38 V) [48], the Ir complex is more difficult to reduce. This indicates that the 4mptr ligand is a weaker π-acceptor than bpy. While for the mononuclear $[M(ppy)_2(NN)]^+$ series, reduction of the anionic ppy ligands usually takes place below −2.3 V [7], the first wave can be assigned to the reduction of the pyridyltriazole ligand. Therefore, the LUMO is centred on the NN ligand. For the rhodium complex, $[Rh(ppy)_2(4mptr)]^+$, the first reduction wave was observed at −1.66 V [27]. Most likely, the second peak at −2.25 V originates from a further reduction of the same 4mptr ligand. Reduction of the ppy ligand(s) can be observed at −2.55 V.

TABLE 5. Electronic and electrochemical data for $[Ir(ppy)_2(4mptr)](PF_6)$

Oxidation[a]	Reduction[a]	Absorption[b]	Emission[c]
1.20	−1.57	460(0.086)	471/505 (77 K)
	−2.15[d]	378(0.54)	582 (r.t.)
	−2.25	267(4.3)	
	−2.55	258(4.2)	

[a]Measured in CH_3CN with 0.1 M NBu_4ClO_4; values in V vs. SCE. [b]Values in nm; measured in EtOH at room temperature (ϵ values in parentheses are in 10^4 M^{-1} cm^{-1}). [c]Measured in propionitrile/butyronitrile (4:5 vol./vol.); values in nm. [d]Shoulder.

Absorption and emission properties

The absorption and emission data are summarised in Table 5. The UV–Vis absorption maxima of the Ir(III) complex are quite similar to those of $[Ir(ppy)_2(bpy)]^+$ as reported by Ohsawa *et al.* [17]. The maximum around 380 nm was assigned as a metal-to-ligand charge transfer (MLCT) band. As for the chloro-bridged dimer $[Ir(ppy)_2Cl]_2$ this maximum was observed at almost the same position [48]; a $d(Ir) \rightarrow \pi^*(ppy)$ transition is present in that region. Furthermore, for the analogous Rh(III) complex, $[Rh(ppy)_2(4mptr)]^+$, the same assignment could be made [27].

The high-energy maxima at 267 and 258 nm originate from ligand-centered (LC) transitions ($\pi \rightarrow \pi^*$) and, compared to literature data [7, 48], can be attributed to intraligand ppy charge transfer. Electronic transitions involving the 4mptr ligand could not be distinguished.

The room temperature emission spectrum shows a broad featureless band with a maximum at 582 nm (Fig. 3). A similar emission band (maximum at 606 nm) has also been observed for the related orthometalated Ir(III) complexes and was assigned as a MLCT concerning the bpy ligand [3, 48]. Therefore, a MLCT band at room temperature for the title compound seems most likely to be attributed to a CT to the pyridyltriazole ligand, although a mixing of MLCT states to the pyridyltriazole and ppy ligand cannot be excluded [48]. The excited-state lifetime of 63 ns supports MLCT assignment. The shift of the maximum to higher energy compared to the bpy analogue can be explained by the weaker π-acceptor properties of the triazole ligands. Due to the higher π^* level of the pyridyltriazole ligands

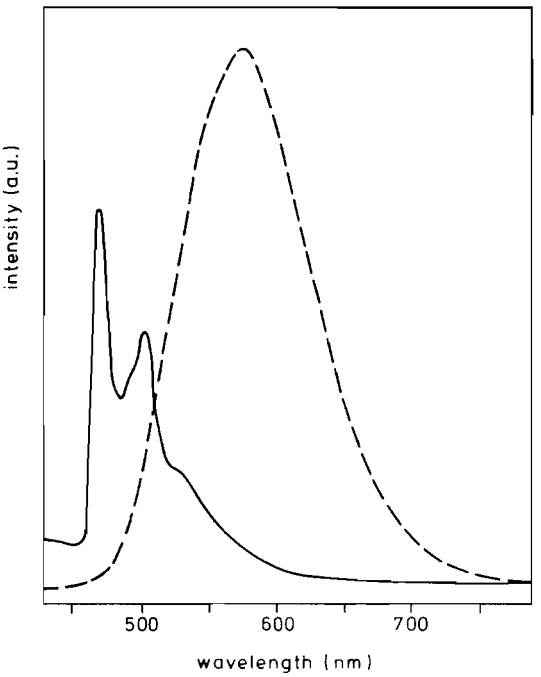

Fig. 3. Emission spectra at 77 K (——), in propionitrile/butyronitrile (4:5 vol./vol.), and at room temperature (– – –) in CH_3CN (5×10^{-5} M) of $[Ir(ppy)_2(4mptr)]^+$.

with respect to bpy it is more difficult to reduce the triazole ligand systems and higher energy MLCT bands are observed.

The spectrum obtained at 77 K revealed two well-resolved maxima at 471 and 505 nm (Fig. 3). Considering the shape of the spectrum a ^{3}LC transition seems to be valid as observed for the rhodium analogues [27]. However, the excited-state lifetime of 2.8 μs found for the title compound is much shorter than the lifetimes (0.16 ms) of the $Rh(ppy)_2$ complexes, for which π–π^* emission was assigned. Furthermore, structured emission features and short lifetimes at 77 K have been observed for other mononuclear Ir(III) complexes and the chloro-bridged dimer, $[Ir(ppy)_2Cl]_2$ [3, 17, 48]. For these compounds MLCT emission has been assigned. These findings suggest that ^{3}MLCT luminescence is most likely present for the $[Ir(ppy)_2(4mptr)]^+$ complex. Detailed lifetime experiments have to reveal if both the orthometalated ppy ligand(s) and the chelating 4mptr ligand are involved in the photophysics at 77 K.

Conclusions

The properties of the orthometalated Ir(III) complex described in this paper are similar to those of the analogous Rh(III) compound. The two ppy ligands are in both cases oriented in a *cis* conformation. Some interesting differences are, however, observed. While Rh(III) complexes generally exhibit only a very weak emission at room temperature, a rather strong luminescence is observed for $[Ir(ppy)_2(4mptr)]^+$ at 300 K. The shape of this maximum and the excited-state lifetime indicate towards a ^{3}MLCT emission dealing with the 4mptr ligand. At 77 K, the emission has most likely also a ^{3}MLCT character.

The electrochemical measurements show that the oxidation process of the Ir(III) centre is observed at much lower potential than observed for the analogous Rh(III) complex. Such behaviour has also been observed for osmium(II) and ruthenium(II) complexes and has been explained by the larger 5d orbitals [49]. The first reduction potentials are in both cases 4mptr based, as the ppy ligands are much more difficult to be reduced. The oxidation and reduction potential show that the π-accepting properties of the 4mptr ligands are weaker than those of bpy. The electrochemical measurements on Ir(III) cyclometalated complexes reveal, therefore, the nature of the ligands unambiguously.

These observations show that the luminescence properties of Ir(III) complexes may be very interesting and in fact such complexes might be of interest for further studies on the ground-state and excited-state properties of d^6 metal complexes.

Acknowledgements

The authors wish to thank Mr S. Gorter for data collection, C. Erkelens and A. W. M. Lefeber for performing the 300 MHz NMR experiments. We gratefully acknowledge Unilever Research Laboratories for permission to use their electrochemical equipment. Emission experiments were performed at Dublin City University. Dr J. G. Vos is thanked for useful discussions.

References

1 M. Nonoyama, *Bull. Chem. Soc. Jpn.*, *47* (1974) 767.
2 M. Nonoyama and S. Kajita, *Transition Met. Chem.*, *6* (1981) 163.
3 S. Sprouse, K. A. King, P. J. Spellane and R. T. Watts, *J. Am. Chem. Soc.*, *106* (1984) 6647.
4 P. Reveco, R. H. Schmehl, W. R. Cherry, F. R. Fronczek and J. Selbin, *Inorg. Chem.*, *24* (1985) 4078.
5 E. C. Constable and J. M. Holmes, *J. Organomet. Chem.*, *301* (1986) 203.
6 K. A. King, P. J. Spellane and R. J. Watts, *J. Am. Chem. Soc.*, *107* (1985) 1531.

7 D. Sandrini, M. Maestri, V. Balzani, U. Maeder and A. von Zelewsky, *Inorg. Chem., 27* (1988) 2640.
8 F. Barigelletti, D. Sandrini, M. Maestri, V. Balzani, A. von Zelewsky, L. Chassot, P. Jolliet and U. Maeder, *Inorg. Chem., 27* (1988) 3644.
9 M. Maestri, D. Sandrini, V. Balzani, A. von Zelewsky and P. Jolliet, *Helv. Chim. Acta, 71* (1988) 134.
10 C. A. Craig and R. J. Watts, *Inorg. Chem., 28* (1989) 309.
11 L. Chassot, E. Muller and A. von Zelewsky, *Inorg. Chem., 23* (1984) 4249.
12 M. Maestri, D. Sandrini, V. Balzani, L. Chassot and P. Jolliet, *Chem. Phys. Lett., 122* (1985) 375.
13 L. Chassot and A. von Zelewsky, *Inorg. Chem., 26* (1987) 2814.
14 C. A. Craig, F. O. Garces, R. J. Watts, R. Palmans and A. J. Frank, *Coord. Chem. Rev., 97* (1990) 193.
15 U. Maeder, J. Jenny and A. von Zelewsky, *Helv. Chim. Acta, 69* (1986) 1085.
16 U. Maeder, *Ph.D. Dissertation,* Fribourg, 1987.
17 Y. Ohsawa, S. Sprouse, K. A. King, M. K. DeArmond, K. W. Hanck and R. J. Watts, *J. Phys. Chem., 91* (1987) 1047.
18 D. Sandrini, M. Maestri, M. Ciano, U. Maeder and A. von Zelewsky, *Helv. Chim. Acta, 73* (1990) 1306.
19 K. A. King and R. J. Watts, *J. Am. Chem. Soc., 109* (1987) 1589.
20 R. Hage, J. G. Hasnoot, J. Reedijk and J. G. Vos, *Inorg. Chim., 118* (1986) 73.
21 R. Hage, R. Prins, J. G. Haasnoot, J. Reedijk and J. G. Vos, *J. Chem. Soc., Dalton Trans.,* (1987) 1389.
22 R. Hage, R. Prins, R. A. G. de Graaff, J. G. Haasnoot, J. Reedijk and J. G. Vos, *Acta Crystallogr., Sect. C, 44* (1988) 56.
23 R. Hage, A. H. J. Dijkhuis, J. G. Haasnoot, R. Prins, J. Reedijk, B. E. Buchanan and J. G. Vos, *Inorg. Chem., 27* (1988) 2185.
24 R. Hage, J. P. Turkenburg, R. A. G. de Graaff, J. G. Haasnoot, J. Reedijk and J. G. Vos, *Acta Crystallogr., Sect. C, 45* (1989) 381; R. Hage, J. G. Haasnoot, D. J. Stufkens, T. L. Snoeck, J. G. Vos and J. Reedijk, *Inorg. Chem., 28* (1989) 1413.
25 F. Barigelletti, L. de Cola, V. Balzani, R. Hage, J. G. Haasnoot, J. Reedijk and J. G. Vos, *Inorg. Chem., 28* (1989) 4344.
26 R. Hage, J. H. van Diemen, G. Ehrlich, J. G. Haasnoot, D. J. Stufkens, T. L. Snoeck, J. G. Vos and J. Reedijk, *Inorg. Chem., 29* (1990) 988.
27 J. H. van Diemen, J. G. Haasnoot, R. Hage, J. Reedijk, J. G. Vos and R. Wang, *Inorg. Chem.,* in press.
28 S. Kubota, M. Uda and M. Ohtsuku, *Chem. Pharm. Bull., 19* (1971) 2331.
29 R. A. G. de Graaff, G. C. Verschoor and S. Gorter, *Program REDDIF83,* Leiden University, 1983.
30 R. A. G. de Graaff, *Acta Crystallogr., Sect. A, 29* (1973) 298.
31 G. M. Sheldrick, *SHELXS86,* program for crystal structure solution, University of Göttingen, F.R.G., 1986.
32 G. M. Sheldrick, *SHELX,* a program for crystal structure determination, University of Cambridge, U.K., 1976.
33 *International Tables for X-ray Crystallography,* Vol. IV, Kynoch Press, Birmingham, U.K., 1974 (present distributor: Kluwer, Dordrecht, The Netherlands).
34 C. K. Johnson, *ORTEP, Rep. ORNL-3794,* Oak Ridge National Laboratory, TN, U.S.A., 1965.
35 A. Zilian, U. Maeder, A. von Zelewsky and H. U. Güdel, *J. Am. Chem. Soc., 111* (1989) 3855.
36 E. C. Constable, T. A. Leese and D. A. Tocher, *Polyhedron, 9* (1990) 1613.
37 A. G. Orpen, L. Brammer, F. H. Allen, O. Kennard, D. G. Watson and R. Taylor, *J. Chem. Soc., Dalton Trans.,* (1989) S1.
38 A. C. Hazell and A. C. Hazell, *Acta Crystallogr., Sect. C, 40* (1984) 806.
39 B. Hubesch, B. Mahieu and J. Meunier-Piret, *Bull. Soc. Chim. Belg., 94* (1985) 685.
40 E. C. Constable, P. R. Raithby and D. N. Smit, *Polyhedron, 8* (1989) 367.
41 D. P. Rillema, D. S. Jones and H. A. Levy, *J. Chem. Soc., Chem. Commun.,* (1979) 849.
42 E. M. Kober, *Ph.D. Thesis,* Chapel Hill, NC, U.S.A., 1982.
43 J. A. Conner, T. J. Meyer and B. P. Sullivan, *Inorg. Chem., 18* (1979) 1388.
44 J. H. van Diemen, M. Biagini-Cingi, J. G. Haasnoot, R. Hage and J. Reedijk, to be published.
45 B. E. Buchanan, R. Wang, J. G. Vos, R. Hage, J. G. Haasnoot and J. Reedijk, *Inorg. Chem., 29* (1990) 3263.
46 R. Hage, J. G. Haasnoot, H. A. Nieuwenhuis, J. Reedijk, D. J. A. de Ridder and J. G. Vos, *J. Am. Chem. Soc., 112* (1990) 9245.
47 J. M. de Wolf, J. G. Haasnoot, R. Hage, J. Reedijk and J. G. Vos, *Nouv. J. Chim.,* in press.
48 F. O. Garces, K. A. King and R. J. Watts, *Inorg. Chem., 27* (1988) 3464.
49 E. M. Kober, J. V. Casper, B. P. Sullivan and T. J. Meyer, *Inorg. Chem., 27* (1988) 4587.